

Article

Complexity of switching chaotic maps in finite precision

M. Antonelli ^{1,2,*} , L. De Micco ^{1,2,3}, H. A. Larondo ^{1,2,3} and O. A. Rosso ^{3,4,5,6}

¹ Facultad de Ingeniería, Universidad Nacional de Mar del Plata (UNMdP), Mar del Plata, Argentina.

² ICyTE. Instituto de Investigaciones Científicas y Tecnológicas en Electrónica.

³ CONICET. Consejo Nacional de Investigaciones Científicas y Técnicas.

⁴ Departamento de Informática en Salud, Hospital Italiano de Buenos Aires, Ciudad Autónoma de Buenos Aires, Argentina.

⁵ Instituto de Física, Universidade Federal de Alagoas (UFAL), Maceió, Brazil.

⁶ Facultad de Ingeniería y Ciencias Aplicadas, Universidad de Los Andes, Santiago, Chile.

* Correspondence: maxanto@fimdp.edu.ar

Academic Editor: name

Version December 29, 2017 submitted to Entropy

Abstract: In this paper we investigate the degradation of the statistic properties of chaotic maps as consequence of their implementation in a digital media such as Digital Signal Processors (DSP), Field Programmable Gate Arrays (FPGA) or Application-Specific Integrated Circuits (ASIC). In these systems, binary floating- and fixed-point are the numerical representations available. Fixed-point representation is preferred over floating-point when speed, low power and/or small circuit area are necessary. Then, in this paper we compare the degradation of fixed-point binary precision version of chaotic maps with the one obtained by using floating point 754-IEEE standard, to evaluate the feasibility of their FPGA implementation. The specific period that every fixed-point precision produces was investigated in previous reports. Statistical characteristics are also relevant, it has been recently shown that it is convenient to describe the statistical characteristic using both, causal and non-causal quantifiers. In this paper we complement the period analysis by characterizing the behavior of these maps from a statistical point of view using quantifiers from information theory. Here, rather than reproducing an exact replica of the real system, the aim is to meet certain conditions related to the statistics of systems.

Keywords: chaos; finite precision; hardware implementaion; switching maps

1. Introduction

In the last years digital systems became the standard in all experimental sciences. By using new programmable electronic devices such as DSP's, ASIC's or FPGA's, experimenters are allowed to design and modify their own signal generators, measuring systems, simulation models, etc.

Nowdays, the chaotic systems are widely used in digital electronics in fields such as electromagnetic compatibility, encrypted secure communications, controlled noise generators, etc [1–6]. These systems are specially interesting due to their extreme sensibility to initial conditions, nevertheless this characteristic is the source of the main difficulties at the time to implement them. In these fields the motivation of using chaotic systems is to generate sequences that meet certain requirements, rather than reproducing an exact replica of the real systems.

When a chaotic system is implemented in computers or any digital device, the chaotic attractor become periodic by the effect of finite precision, then only pseudo chaotic attractors can be generated [7,8]. Discretization may even destroy the pseudo chaotic behavior and consequently is a non trivial process [3,9].

30 In these new devices, floating- and fixed-point are the available arithmetic. Floating-point is the
31 more accurately solution but is not always recommended when speed, low power and/or small circuit
32 area are required. A fixed-point solution is better in these cases, nevertheless the feasibility of their
33 implementation needs to be investigated.

34 The effect of numerical discretization over a chaotic map was recently addressed in [7], [3] and
35 [10]. In our previous work [3] we have explored the statistical degradation of the phases' space for
36 a family of 2D quadratic maps. These maps present a multiatractor dynamic that makes them very
37 attractive as random number generator in fields like criptography, encoding, etc. Nepomuceno *et al.*
38 [10] reported the existence of more than one pseudo-orbit of continuous chaotic systems when it is
39 discretized using different schemes.

40 Grebogi and coworkers [11] saw that the period T scales with roundoff ϵ as $T \sim \epsilon^{-d/2}$ where
41 d is the correlation dimension of the chaotic attractor. This issue was also addressed in [12], in this
42 paper authors explore the evolution on the period T as consequence of roundoff induced by 2-based
43 numerical representation. To have a large period T is an important property of chaotic maps, in
44 [13] Nagaraj *et. al* studied the effect of switching over the average period lengths of chaotic maps in
45 finite precision. They saw that the period T of the compound map obtained by switching between
46 two chaotic maps is higher than the period of each map. Liu *et. al* [14] studied different switching
47 rules applied to linear systems to generate chaos. Switching issue was also addressed in [15], the
48 author considered some mathematical, physical and engineering aspects related to singular, mainly
49 switching systems. Switching systems naturally arise in power electronics and many other areas in
50 digital electronics. They have also interest in transport problems in deterministic ratchets [16] and it is
51 known that synchronization of the switching procedure affects the output of the controlled system.
52 Chiou and Chen [17] published an analysis of the stabilization and switching laws to design switched
53 discrete-time systems. Recently, Borah *et al.* [18] presented a family of new chaotic systems and a
54 switching based synchronization strategy.

55 Stochasticity and mixing are relevant to characterize a chaotic behavior. To investigate these
56 properties several quantifiers were studied [19]. Entropy and complexity from information theory
57 were applied to give a measure for causal and non causal entropy and causal complexity.

58 A fundamental issue is the criterium to select the probability distribution function (PDF) assigned
59 to the time series, causal and non causal options are possible. Here we consider the non causal
60 traditional PDF obtained by normalizing the histogram of the time series. Its statistical quantifier is
61 the normalized entropy H_{hist} that is a measure of equiprobability among all allowed values. We also
62 considered a causal PDF that is obtained by assigning ordering patterns to segments of trajectory of
63 length D . This PDF was first proposed by Bandt & Pompe in a seminal paper [20], the corresponding
64 entropy H_{BP} was also proposed as a quantifier by Bandt & Pompe. In [23] authors applied the
65 causal complexity C_{BP} to detect chaos. Among them the use of an entropy-complexity representation
66 ($H_{hist} \times C_{BP}$ plane) and causal-non causal entropy ($H_{BP} \times H_{hist}$ plane) deserves special consideration
67 [19,21–25].

68 Recently, amplitude information was introduced in [26] to add some immunity to weak noise in a
69 causal PDF. The new scheme better tracks abrupt changes in the signal and assigns less complexity to
70 segments that exhibit regularity or are subject to noise effects. Then, we define the causal entropy with
71 amplitude contributions H_{BPW} and the causal complexity with amplitude contributions C_{BPW} . Also,
72 we introduce the modified planes $H_{hist} \times C_{BP}$ and $H_{BP} \times H_{hist}$.

73 Amigó and coworkers proposed the number of forbidden patterns as a quantifier of chaos [27].
74 Essentially they reported the presence of forbidden patterns as an indicator of chaos. Recently it was
75 shown that the name forbidden patterns is not convenient and it was replaced by missing patterns
76 (MP) [28], in this work authors showed that there are chaotic systems that present MP from a certain
77 minimum length of patterns. Our main interest on MP is because it gives an upper bound for causal
78 quantifiers.

Following [13], in this paper we study the statistical characteristics of five maps, two well known maps: (1) the tent (TENT) and (2) logistic (LOG) maps, and three additional maps generated from them: (3) SWITCH, generated by switching between TENT and LOG; (4) EVEN, generated by skipping all the elements in odd positions of SWITCH time series and (5) ODD, generated by discarding all the elements in even positions of SWITCH time series. Binary floating- and fixed-point numbers are used, these specific numerical systems may be implemented in modern programmable logic devices.

The main contribution of this paper is the study of how different statistical quantifiers detect the evolution of stochasticity and mixing of the chaotic maps according as the numerical precision varies. To illustrate this sequences generated by well known maps were used, and also sequences obtained by randomization methods like skipping and switching.

Organization of the paper is as follows: Section 2 describes the statistical quantifiers used in the paper and the relationship between their value and the characteristics of the causal and non causal PDF's considered; Section 3 shows and discusses the results obtained for all the numerical representations. Finally Section 4 deals with final remarks and future work.

2. Information theory quantifiers

Systems that evolve over time are called dynamical systems. Generally, only measurements of scalar time series $X(t)$ are accessible, these time series may be function of variables $V = \{v_1, v_2, \dots, v_k\}$ describing the underlying dynamics (i.e. $dV/dt = f(V)$). The goal is to infer properties and reach conclusions of an unknown system from the analysis of measured record of observational data. The key question would be to know how much information about the dynamics of the underlying processes can be revealed by the analyzed data. A probability distribution function (PDF) P is typically used to quantify the apportionment of a time series $X(t)$. Information Theory quantifiers can be defined as measures that characterize properties of the PDF associated with these time series, they allow to extract information about the studied system. We can see these quantifiers as metrics in the PDFs space, they enable to compare and classify different sets of data according to their PDFs where stochastic and deterministic are the two extremes of processes.

Here, we are concerned in chaotic dynamics, which are fundamentally *causal* and *statistical* in nature. For this reason, we are forced to use a different approach since a purely statistical approach ignores the correlations between successive values from the time series; and a causal approach focuses on the PDFs of data sequences.

The selected quantifiers are based on symbolic counting and ordinal pattern statistics. They make it possible to distinguish between the two main features: the *information content* of data and their *complexity*. It is important to highlight that rather than referring to a physical space, here we talk about a space of probability density functions.

In this section, we will introduce Information Theory quantifiers defined over discrete PDFs since discrete time series is our scope. Nevertheless, in [29] definitions for the continuous case can be found.

2.1. Shannon entropy and statistical complexity

Entropy is a measure of the uncertainty associated with a physical process that is described by P . The Shannon entropy is considered as the most natural one [29] when dealing with information content.

Let define a discrete probability distribution $P = \{p_i; i = 1, \dots, N\}$ with $\sum_{i=1}^N p_i = 1$, were N is the number of possible states of the system under study. Then, Shannon's logarithmic information measure:

$$S[P] = - \sum_{i=1}^N p_i \ln [p_i] \quad (1)$$

When $S[P] = S_{\min} = 0$, the prediction of which outcome i will occur is a complete certainty. In this case, it is maximal the knowledge of the underlying process described by the probability distribution. On the contrary, we have minimal knowledge in a case of a uniform distribution

$P_e = \{p_i = 1/N; i = 1, \dots, N\}$ since every outcome has the same probability of occurrence, and the uncertainty is maximal, i.e., $S[P_e] = S_{\max} = \ln N$. These two situations are extreme cases, therefore we focus on the ‘normalized’ Shannon entropy, $0 \leq H \leq 1$, given as

$$H[P] = S[P]/S_{\max} \quad (2)$$

On the other hand, there is not a unique definition of the concept of complexity. In this paper, the aim is to describe the complexity of the time series rather than that of the underlying systems. As stated by Kantz [30], complex data might be generated by “simple” systems, while “complicated” models can generate low complexity outputs. A quantitative complexity can be defined as a measure that assigns low values both to uncorrelated random data (maximal Shannon entropy) and also to perfectly ordered data (null Shannon entropy). Then, if we have an ordered sequence, such as a simple oscillation or trend, the statistical complexity would be low, and the same would happen with an unordered sequence, such as uncorrelated white noise. In the middle of this situation the characterization of data is more difficult hence the complexity would be higher.

We look forward a quantifier functional of a PDF, $C[P]$, in order to measure the degree of complexity or of correlational structures. As depicted in [31] the functional is relate to organization, correlational structure, memory, regularity, symmetry, patterns, and other properties.

Rosso and coworkers [32] introduced a suitable *Statistical Complexity Measure* (SCM) C , that is based on the seminal notion advanced by López-Ruiz *et al.* [33]. SCM is defined as the product of a measure of information and a measure of disequilibrium and it is able to detect the distance from the equiprobable distribution of the accessible states.

This statistical complexity measure [32,34] is defined as follows:

$$C[P] = Q_J[P, P_e] \cdot H[P] \quad (3)$$

H is the normalized Shannon entropy, see eq. 2, and Q_J is the disequilibrium defined in terms of the Jensen-Shannon divergence $J[P, P_e]$, [35]. That is,

$$Q_J[P, P_e] = Q_0 J[P, P_e] = Q_0 \{S[(P + P_e)/2] - S[P]/2 - S[P_e]/2\} \quad (4)$$

Q_0 is a normalization constant such that $0 \leq Q_J \leq 1$:

$$Q_0 = -2 \left\{ \frac{N+1}{N} \ln(N+1) - \ln(2N) + \ln N \right\}^{-1} \quad (5)$$

This value is obtained in a totally deterministic situation, where only one components of P has a no null value equal to one.

Note that the above introduced SCM depends on two different probability distributions: one associated with the system under analysis, P , and the other with the uniform distribution, P_e . Furthermore, it was shown that for a given value of H , the range of possible C values varies between a minimum C_{\min} and a maximum C_{\max} , restricting the possible values of the SCM [36]. Thus, it is clear that important additional information related to the correlational structure between the components of the physical system is provided by evaluating the statistical complexity measure.

2.2. Determination of a probability distribution

The evaluation derived from the Information Theory quantifiers suppose some prior knowledge about the system; specifically for those previously introduced (Shannon entropy and statistical complexity), a probability distribution associated to the time series under analysis should be provided before. The determination of the most adequate PDF is a fundamental problem because the PDF P and the sample space Ω are inextricably linked. Usual methodologies assign to each value of the series $X(t)$ (or non-overlapped set of consecutive values) a symbol from a finite alphabet $A = \{a_1, \dots, a_M\}$,

thus creating a *symbolic sequence* that can be regarded to as a *non causal coarse grained* description of the time series under consideration. In this case, information on the dynamics of the system is lost, such as order relations and the time scales.

If we want to incorporate *Causal information* we have to add information about the past dynamics of the system, this is done by the assignment of symbols of alphabet A to a portion of the trajectory. The Bandt and Pompe (BP) [20] method is a simple and robust methodology that compares neighboring values in a time series and, thus solves this issue. The causality property of the PDF allows quantifiers (based on this PDFs) to discriminate between deterministic and stochastic systems [37]. The steps are, first it is needed to create symbolic data by ranking the values of the series; and second to define by reordering the embedded data in ascending order. This last step is the same to make a phase space reconstruction, using embedding dimension D (pattern length) and time lag τ . The goal of quantifying the diversity of the ordering symbols is achieved. There is no need to perform model-based assumptions, because the appropriate symbol sequence arises naturally from the time series.

The procedure is the following:

- Given a series $\{x_t; t = 0, \Delta t, \dots, N\Delta t\}$, a sequence of vectors of length D is generated.

$$(s) \longmapsto (x_{t-(d-1)\Delta t}, x_{t-(d-2)\Delta t}, \dots, x_{t-\Delta t}, x_t) \quad (6)$$

Each vector turns out to be the “history” of the value x_t . Clearly, the longer the length of the vectors D , the more information about the history would the vectors have but a higher value of N is required to have an adequate statistics.

- The permutations $\pi = (r_0, r_1, \dots, r_{D-1})$ of $(0, 1, \dots, D-1)$ are called “order of patterns” of time t , defined by:

$$x_{t-r_{D-1}\Delta t} \leq x_{t-r_{D-2}\Delta t} \leq \dots \leq x_{t-r_1\Delta t} \leq x_{t-r_0\Delta t} \quad (7)$$

In order to obtain an unique result it is considered $r_i < r_{i-1}$ if $x_{t-r_i\Delta t} = x_{t-r_{i-1}\Delta t}$. In this way, all the $D!$ possible permutations π of order D , and the PDF $P = \{p(\pi)\}$ is defined as:

$$p(\pi) = \frac{\#\{s | s \leq N - D + 1; (s) \text{ has type } \pi\}}{N - D + 1} \quad (8)$$

In the last expression the $\#$ symbol denotes cardinality.

From the time series an ordinal pattern probability distribution $P = \{p(\pi_i), i = 1, \dots, D!\}$ is extracted. For this, a unique symbol π is obtained from the vector defined by eq. 8. For uniqueness, $r_i < r_{i-1}$ if $x_{s-r_i} = x_{s-r_{i-1}}$ is defined. With the following stationary assumption: for $k \leq D$, the probability for $x_t < x_{t+k}$ should not depend on t need to be met for the applicability of the BP method. Regarding the selection of the parameters, Bandt and Pompe suggested working with $3 \leq D \leq 6$ for typical time series lengths, and specifically considered a time lag $\tau = 1$ in their cornerstone paper.

Recently, the permutation entropy was extended to incorporate amplitude information. In order to avoid the loss of amplitude information, that would be a disadvantage of ordinal pattern statistics, weights are introduced to obtain a “weighted permutation entropy (WPE)” [26]. Non-normalized weights are computed for each temporal window for the time series X , such that

$$w_j = \frac{1}{D} \sum_{k=1}^D (x_{j+k-1} - \bar{X}_j^D)^2 \quad (9)$$

In the equation above $x_{j+k-1} - \bar{X}_j^D$ denotes the arithmetic mean of the current embedding vector of length D and its variance w_j is then used to weight the relative frequencies of each ordinal pattern p_j . Originally, this technique was proposed to discriminate patterns immersed in low noise. We take advantage of the fact that the fixed points are not computed in the WPE.

178 We calculated the normalized permutation Shannon entropy H and the statistical complexity C
 179 from these PDFs, and the obtained values are denoted as:

- 180 • H_{hist} , is the normalized Shannon entropy applied to non-causal PDF P_{hist}
- 181 • H_{BP} , is the normalized Shannon entropy applied to causal PDF P_{BP}
- 182 • H_{BPW} , is the normalized Shannon entropy applied to causal PDF with amplitude contribution
 P_{BPW}
- 184 • C_{BP} , is the normalized statistical complexity applied to causal PDF P_{BP}
- 185 • C_{BPW} , is the normalized statistical complexity applied to causal PDF with amplitude contribution
 P_{BPW}

187 *2.3. Information Planes*

188 A particularly useful visualization of the quantifiers from Information Theory is their juxtaposition
 189 in two-dimensional graphs. These diagnostic tools were shown to be particularly efficient to distinguish
 190 between the deterministic chaotic and stochastic nature of a time series since the permutation
 191 quantifiers have distinct behaviors for different types of processes. Four information planes are
 192 defined:

- 193 1. Causal entropy vs. non-causal entropy, $H_{BP} \times H_{hist}$
- 194 2. Causal entropy with amplitude contributions vs. non-causal entropy, $H_{BPW} \times H_{hist}$
- 195 3. Causal causal complexity vs. causal entropy, $C_{BP} \times H_{BP}$
- 196 4. Causal causal complexity with amplitude contributions vs. causal entropy with amplitude
 contributions, $C_{BPW} \times H_{BPW}$

198 In Figure 1 we show the planes $H_{BP} \times H_{hist}$ and $H_{BPW} \times H_{hist}$ overlapped. In the resulting plane
 199 a higher value in any of the entropies, H_{BP} , H_{BPW} or H_{hist} , implies a more uniformity in the involved
 200 PDF. The point (1, 1) represents the ideal case with uniform histogram and uniform distribution of
 201 ordering patterns. We show some relevant points as example. Ideal white random sequences with
 202 uniform distribution gives a point at $(H_{hist}, H_{BP}) = (1, 1)$ represented by a blue circle, a red circle in
 203 the same position shows the results when amplitude contributions are included $(H_{hist}, H_{BPW}) = (1, 1)$.
 204 If we sort the vector generated by ideal white random generator in an ascendant way, resulting points
 205 are shown by a blue square $(H_{hist}, H_{BP}) = (1, 0)$ and a red square $(H_{hist}, H_{BPW}) = (1, 0)$, in both
 206 cases the squares are overlapped at point (1, 0) this example illustrates the complementarity of the
 207 information provided by H_{hist} and H_{BP} .

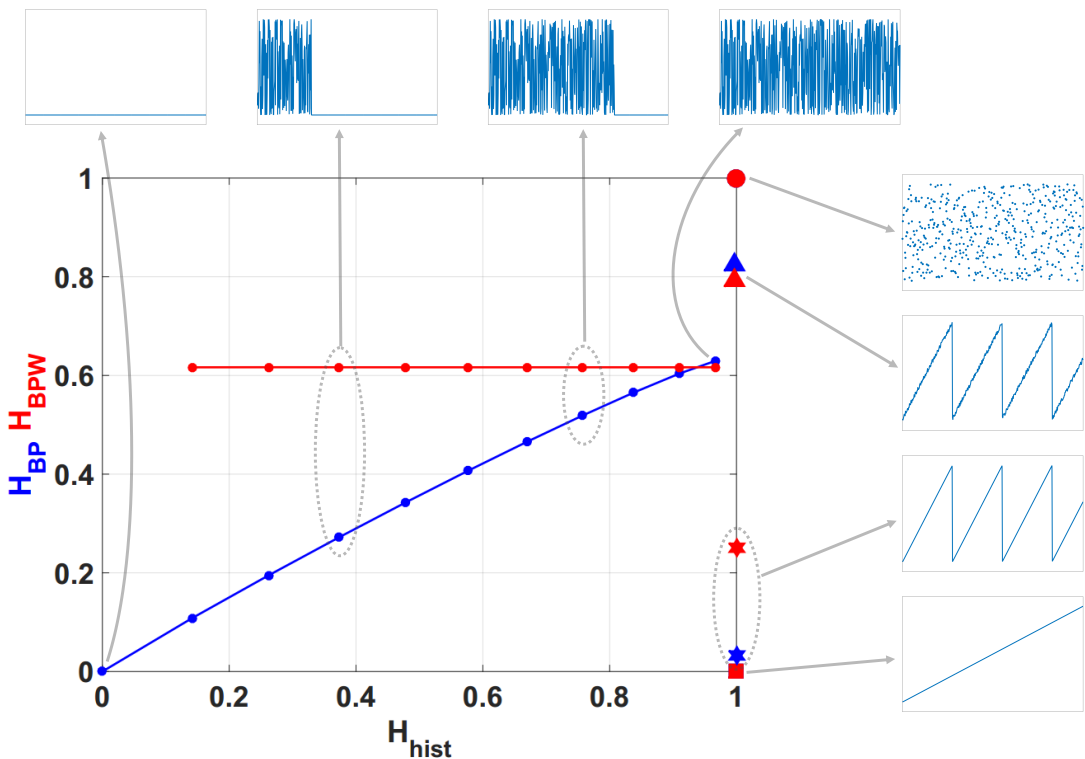


Figure 1. Causal-Non causal Entropy plane, values of the quantifiers for some characteristic signals, from purely deterministic through purely random (see text).

208 Blue and red stars show (H_{hist}, H_{BP}) and (H_{hist}, H_{BPW}) respectively, applied to a sawtooth signal.
 209 Values are perfectly distributed in all interval but only a few ordering patterns appear, this explains the
 210 high H_{hist} and low H_{BP} . The frequency of occurrence of low amplitude patterns is higher than the one
 211 of high amplitude patterns, then the PDF with amplitude contributions is more uniform and H_{BPW} is
 212 a little higher than H_{BP} . When sawtooth signal is contaminated with white noise H_{BP} and H_{BPW} are
 213 increased as shown with blue and red triangles. Clearly, new ordering patterns appear and both H_{BP}
 214 and H_{BPW} show higher values than non-contaminated case. However the growth of H_{BPW} is smaller
 215 than H_{BP} showing that the technique of recording amplitude contributions adds some immunity to
 216 noise.

217 Finally, we evaluated the quantifiers for a sequence of a logistic map that converges to a fixed point,
 218 in all cases the length of data vector remains constant and the length of transitory is variable. Results
 219 obtained without amplitude contributions are depicted in blue dots, they converge to $(H_{hist}, H_{BP}) =$
 220 $(0, 0)$ as the length of transitory is shorter, however H_{BPW} (in red points) remains constant for all the
 221 cases. The last point in $(H_{hist}, H_{BP}) = (0, 0)$ corresponds to a vector of zeros, in this case the histogram
 222 of ordering patterns with amplitude contributions is also a zero vector and H_{BPW} can not be calculated.
 223 Through this last example, we show that the convergence to a fixed point can be detected by the joint
 224 information of H_{BP} and H_{BPW} .

225 In Figure 2 we show the causality plane $H_{BP} \times C_{BP}$ with and without amplitude contributions.
 226 The same sample points are showed to illustrate the planar positions for different data vectors. We can
 227 see that not the entire region $0 < H_{BP} < 1, 0 < C_{BP} < 1$ is achievable, in fact, for any PDF the pairs
 228 (H, C) of possible values fall between two extreme curves in the plane $H_{BP} \times C_{BP}$ [38].

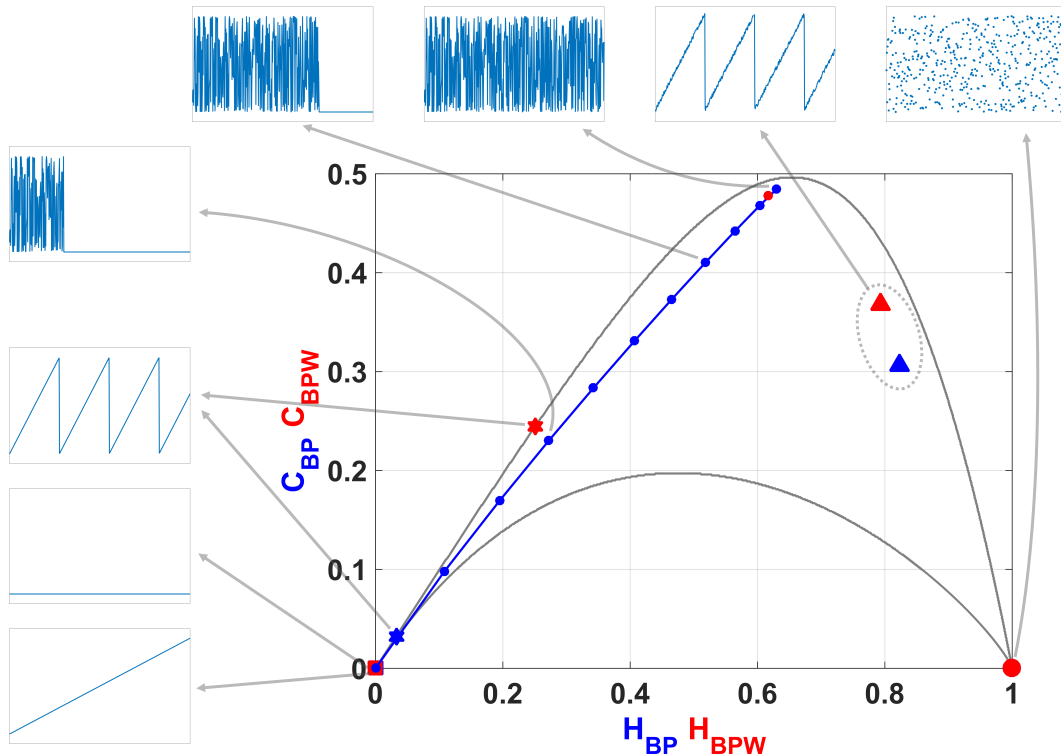


Figure 2. Causal Entropy-Complexity plane, values of the quantifiers for some characteristic signals, from purely deterministic through purely random (see text).

229 Chaotic maps present high values of complexity C_{BP} (close to the upper complexity limit), and
 230 intermediate entropy H_{BP} [23,39]. In the case of regular processes the values of entropy and complexity
 231 are close to zero. Stochastic processes that are uncorrelated present H_{BP} near one and C_{BP} near zero.
 232 Ideal random systems having uniform Bandt & Pompe PDF, are represented by the point $(1, 0)$ [40]
 233 and a delta-like PDF corresponds to the point $(0, 0)$. In both information planes $H_{BP} \times H_{hist}$ in Figure
 234 1 and $H_{BP} \times C_{BP}$ in Figure 2, stochastic, chaotic and deterministic data are clearly localized at different
 235 planar positions.

236 We also used the number of missing patterns MP as a quantifier [28]. As shown recently by Amigó
 237 *et al.* [41–44], in the case of deterministic maps, not all the possible ordinal patterns can be effectively
 238 materialized into orbits. Thus, for a fixed pattern-length (embedding dimension D) the number of
 239 missing patterns of a time series (unobserved patterns) is independent of the series length N . Remark
 240 that this independence does not characterize other properties of the series such as proximity and
 241 correlation, which die out with time [42,44]. In this paper, we use the MP to calculate an upper bound
 242 to the H_{BP} and H_{BPW} .

243 A complete description and discussion about these quantifiers is out of scope of this manuscript.
 244 However, it can be found in [21,24,28,33,36,45–47].

245 3. Results

246 Five pseudo chaotic maps were studied, two simple maps and three combination of them. For
 247 each one we have used numbers represented by floating-point (double precision 754-IEEE standard)
 248 and fixed-point numbers with $1 \leq B \leq 53$, where B is the number of bits that represents the fractional
 249 part. Time series were generated using 100 randomly chosen initial conditions within their attraction
 250 domain (interval $[0, 1]$), for each one of these 54 number precisions. The studied maps are logistic

²⁵¹ (LOG), tent (TENT), sequential switching between TENT and LOG (SWITCH) and skipping discarding
²⁵² the values in the odd positions (EVEN) or the values in the even positions (ODD) respectively.

Logistic map is interesting because it is representative of the very large family of quadratic maps.
 Its expression is:

$$x_{n+1} = 4x_n(1 - x_n) \quad (10)$$

²⁵³ with $x_n \in \mathbb{R}$.

Note that to effectively work in a given representation it is necessary to change the expression of the map in order to make all the operations in the chosen representation numbers. For example, in the case of LOG the expression in binary fixed-point numbers is:

$$x_{n+1} = 4\epsilon \text{ floor} \left\{ \frac{x_n(1 - x_n)}{\epsilon} \right\} \quad (11)$$

²⁵⁴ with $\epsilon = 2^{-B}$ where B is the number of bits that represents the fractional part.

²⁵⁵ Floating point representation does not constitute a field, wherein the basic maths properties, such
²⁵⁶ as distributive, associative, are preserved. However, in fixed point arithmetics the exponent does not
²⁵⁷ shift the point position and some properties as distributive remains. Also, we adopt the floor rounding
²⁵⁸ mode because it arises naturally in a FPGA implementation.

²⁵⁹ The TENT map has been extensively studied in the literature because theoretically it has nice
²⁶⁰ statistical properties that can be analytically obtained. For example it is easy to proof that it has
²⁶¹ a uniform histogram and consequently an ideal $H_{hist} = 1$. The Perron-Frobenius operator and its
²⁶² corresponding eigenvalues and eigenfunctions may be analytically obtained for this map [48].

Tent map is represented with the equation:

$$x_{n+1} = \begin{cases} 2x_n & , \text{if } 0 \leq x_n \leq 1/2 \\ 2(1 - x_n) & , \text{if } 1/2 < x_n \leq 1 \end{cases} \quad (12)$$

²⁶³ with $x_n \in \mathbb{R}$.

In base-2 fractional numbers rounding, equation (12) becomes:

$$x_{n+1} = \begin{cases} 2x_n & , \text{if } 0 \leq x_n \leq 1/2 \\ \epsilon \text{ floor}\left\{ \frac{2 - 2x_n}{\epsilon} \right\} & , \text{if } 1/2 < x_n \leq 1 \end{cases} \quad (13)$$

²⁶⁴ with $\epsilon = 2^{-B}$.

²⁶⁵ In this case, we introduce the 2 number in the parentheses because it is computationally more
²⁶⁶ efficient in a hardware implementation. It is valid because it is power of 2 and the multiplication is
²⁶⁷ equivalent to a shift-to-left.

²⁶⁸ Switching, even and odd skipping procedures are shown in Fig. 3.

SWITCH map is expressed as:

$$\begin{cases} x_{n+1} = \begin{cases} 2x_n, & , \text{if } 0 \leq x_n \leq 1/2 \\ 2(1 - x_n) & , \text{if } 1/2 < x_n \leq 1 \end{cases} \\ x_{n+2} = 4x_{n+1}(1 - x_{n+1}) \end{cases} \quad (14)$$

²⁶⁹ with $x_n \in \mathbb{R}$ and n an even number.

²⁷⁰ Skipping is a usual randomizing technique that increases the mixing quality of a single map
²⁷¹ and correspondingly increases the value of H_{BP} and decreases C_{BP} of the time series. Skipping does
²⁷² not change the values of H_{hist} for ergodic maps because it are evaluated using the non causal PDF
²⁷³ (normalized histogram of values) [21].

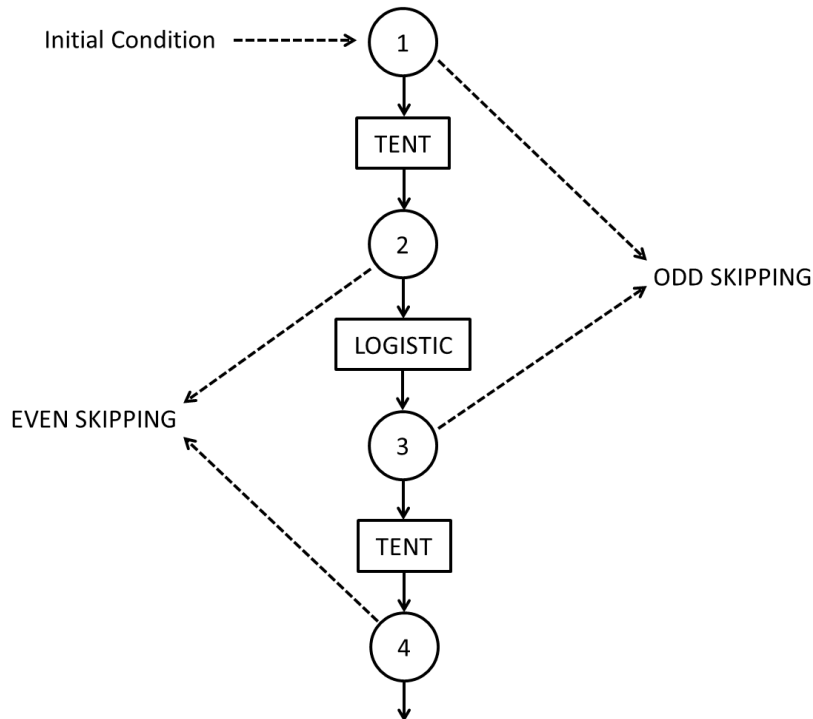


Figure 3. Sequential switching between Tent and Logistic maps. In the figure are also shown even and odd skipping strategies.

274 In the case under consideration we study even and odd skipping of the sequential switching of
 275 TENT and LOG maps:

- 276 1. Even skipping of the sequential switching of Tent and Logistic maps (EVEN).
 277 If $\{x_n; n = 1, \dots, \infty\}$ is the time series generated by eq. (14), discard all the values in odd positions
 278 and retain the values in even positions.
 279 2. Odd skipping of the sequential switching of Tent and Logistic maps. If $\{x_n; n = 1, \dots, \infty\}$ is the
 280 time series generated by eq. (14), discard all the values in even positions and retain all the values
 281 in odd positions.

282 Even skipping may be expressed as the composition function $\text{TENT} \circ \text{LOG}$ while odd skipping
 283 may be expressed as $\text{LOG} \circ \text{TENT}$. The evolution of period as function of precision was reported in [13]
 284 for these resulting maps.

285 3.1. Period as a function of binary precision

286 Grebogi and coworkers [11] have studied how the period T is related with the precision. There
 287 they saw that the period T scales with roundoff ϵ as $T \sim \epsilon^{-d/2}$ where d is the correlation dimension of
 288 the chaotic attractor.

289 Nagaraj *et al.* [13] studied the case of switching between two maps. They saw that the period T
 290 of the compound map obtained by switching between two chaotic maps is higher than the period of
 291 each map and they found that a random switching improves the results. Here we have considered
 292 sequential switching to avoid the use of another random variable, because it can include its own
 293 statistical properties in the time series.

294 Figure 4 shows T vs. B in semi logarithmic scale. We run the attractor of the LOG from 100
 295 randomly chosen initial conditions. The figure show: 100 red points for each fixed-point precision
 296 ($1 \leq B \leq 53$) and their average (dashed black line connecting black dots). The experimental averaged

²⁹⁷ points can be fitted by a straight line (in blue) expressed as $\log_{10} T = mB + b$ where m is the slope and
²⁹⁸ b is the y -intercept. Results for all the considered maps are summarized in Table 1.

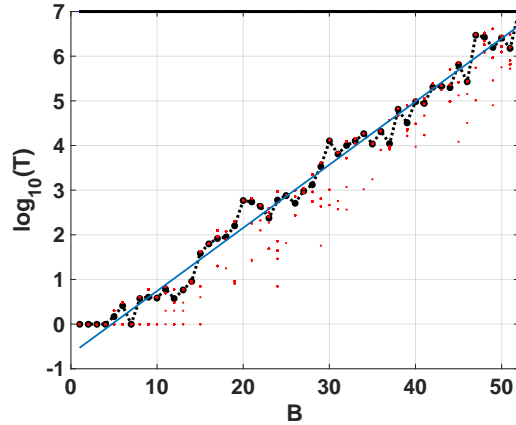


Figure 4. Period as function of precision in binary digits (see text).

Table 1. Period T as a function of B for the maps considered

map	m	b
TENT	0	0
LOG	0.139	-0.6188
SWITCH	0.1462	-0.5115
EVEN	0.1447	-0.7783
ODD	0.1444	-0.7683

²⁹⁹ Results are compatible for those obtained in [13]. Switching between maps increases the period T
³⁰⁰ but skipping procedure decreases by almost half.

³⁰¹ 3.2. Quantifiers of simple maps

³⁰² Here we report our results for both simple maps, LOG and TENT

³⁰³ 3.2.1. LOG

³⁰⁴ Figures 5a to 5f show the statistical properties of LOG map in floating-point and fixed-point
³⁰⁵ representation. All these figures show: 100 red points for each fixed-point precision ($1 \geq B \geq 53$) and
³⁰⁶ in black their average (dashed black line connecting black dots), 100 horizontal dashed blue lines that
³⁰⁷ are the results of each run in floating-point and a black solid line their average. Note that these lines
³⁰⁸ are independent of x-axis. In this case, all the lines of the floating-point are overlapped.

³⁰⁹ According as B grows, statistical properties vary until they stabilize. For $B \geq 30$ the value of
³¹⁰ H_{hist} remains almost identical to the value for the floating-point representation whereas H_{BP} and C_{BP}
³¹¹ stabilizes at $B > 21$. Their values are: $\langle H_{hist} \rangle = 0.9669$; $\langle H_{BP} \rangle = 0.6269$; $\langle C_{BP} \rangle = 0.4843$. Note that the
³¹² stable value of missing patterns $MP = 645$ makes the optimum $H_{BP} \leq \ln(75) / \ln(720) \simeq 0.65$. Then,
³¹³ $B = 30$ is the most convenient choice for hardware implementation because an increase in the number
³¹⁴ of fractional digits does not improve the statistical properties.

³¹⁵ Some conclusions can be drawn regarding BP and BPW quantifiers. For $B = 1, 2, 3$ and 4, the
³¹⁶ averaged BP quantifiers are almost 0 while the averaged BPW quantifiers can not be calculated (see in
³¹⁷ Figures 5c and 5e the missing black dashed line). This is because for those sequences were the initial

³¹⁸ condition were 0 all iterations result to be a sequence of zeros (the fixed point of the map), this is more
³¹⁹ likely to happen when using small precisions because of roundoff.

³²⁰ When B increases the initial conditions are rounded to zero less frequently, this can be seen for
³²¹ $B > 6$. In this, case the generated sequences starting from a non-null value fall to zero after a short
³²² transitory very often. An interesting issue in Figures 5c and 5e, is that BPW quantifiers show a high
³²³ dispersion unlike BP quantifiers. This is because BPW procedure takes into account the transient and
³²⁴ discards fixed points, unlike BP procedure considers all the values of the sequence. We can see in
³²⁵ Figures 5c and 5e for $1 < B < 10$ horizontal lines of red points that do not appear in Figures 5b and 5d,
³²⁶ this evidences that different initial conditions fall to the same orbits, even for adjacent precisions.

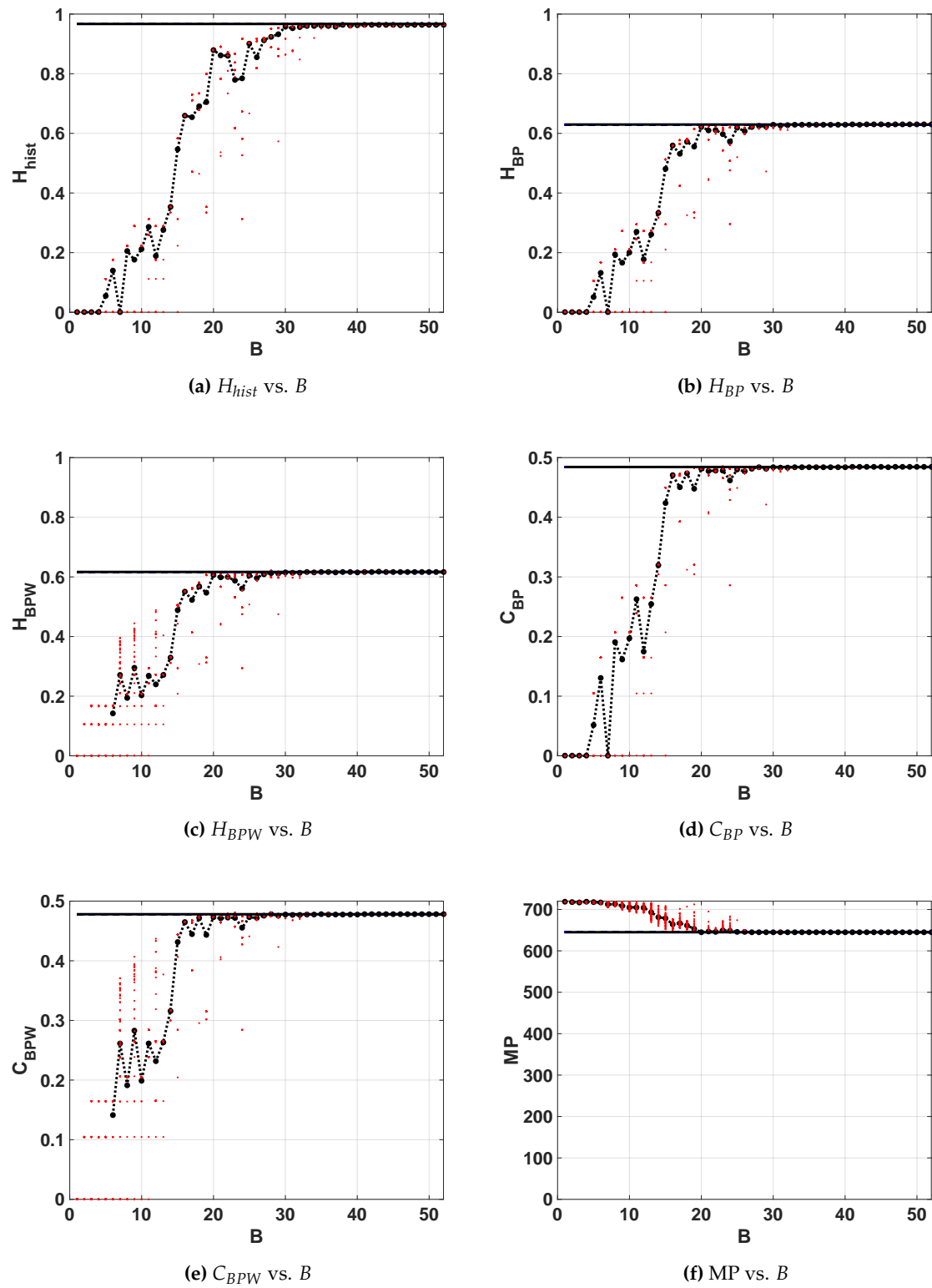


Figure 5. Statistical properties for LOG map as function of B .

327 The same results are shown in double entropy planes with the precision as parameter (Figure 6a
 328 without amplitude contributions and Figure 6b with amplitude contributions). These figures show: 100
 329 red points for each fixed-point precision (B) and their average in black (dashed black line connecting

330 black dots), 100 blue dots that are the results of each run in floating-point and the black star is their
331 average. Here, the 100 blue points and their average are overlapped.

As expected, the fixed-point architecture implementation converges to the floating-point value as B increases. For both planes, $H_{hist} \times H_{BP}$ and $H_{hist} \times H_{BPW}$, from $B = 20$, H_{hist} increases but H_{BP} and H_{BPW} remain constant. It can be seen that the distribution of values reaches high values ($\langle H_{hist} \rangle = 0.9669$) but their mixing is poor ($\langle H_{BP} \rangle = 0.6269$).

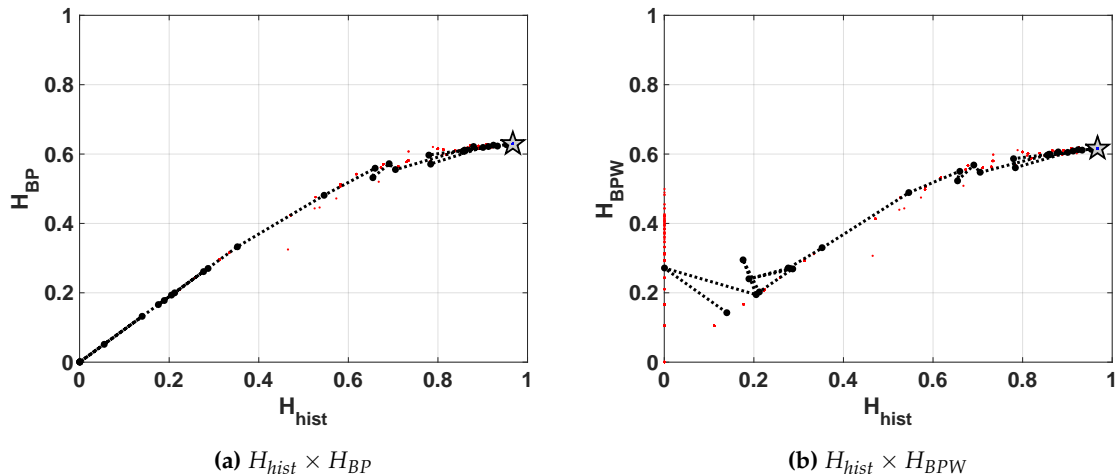


Figure 6. Evolution of statistical properties in double entropy plane for LOG map.

In Figure 7a and 7b we show the entropy-complexity planes. Dotted gray lines are the upper and lower margins, it is expected that a chaotic system remains near the upper margin. These results characterize a chaotic behavior, in $H_{BP} \times C_{BP}$ plane we can see a low entropy and high complexity.

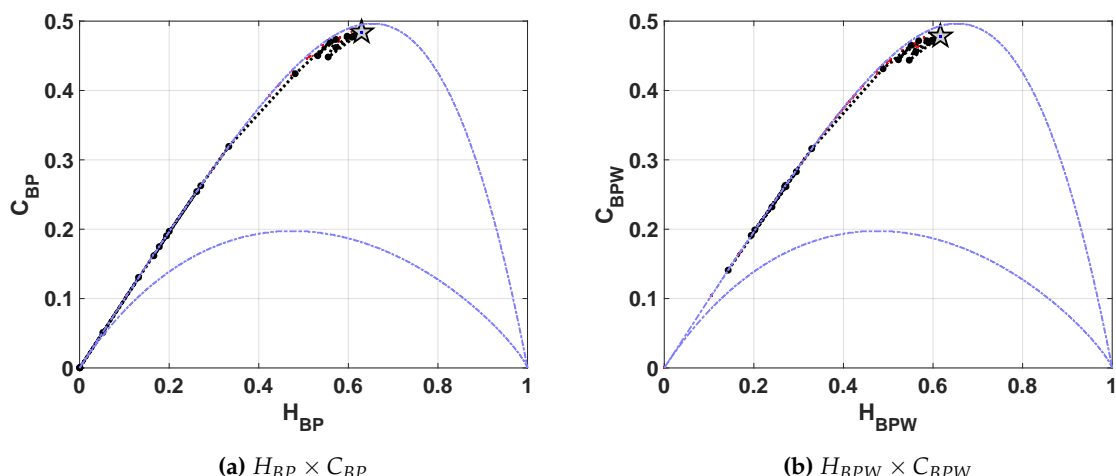


Figure 7. Evolution of statistical properties in causal entropy-complexity plane for LOG map.

339 3.2.2. TENT

When this map is implemented in a computer using any numerical representation system (even floating-point!) truncation errors rapidly increase and make unstable fixed point in $x^* = 0$ to become stable. The sequences within the attractor domain of this fixed point will have a short transitory of length between 0 and B followed by an infinite number of 0's [49,50]. This issue is easily explained in

[51], the problem appears because all iterations have a left-shift operation that carries the 0's from the right side of the number to the most significant positions.

Figures 8a to 8f show the quantifiers for floating- and fixed-point numerical representations. H_{hist} , H_{BP} and C_{BP} quantifiers are equal to zero for all precisions, this reflects that the series quickly converge toward a fixed point for every initial conditions. In the case of H_{BPW} and C_{BPW} quantifiers are different to zero because BPW procedure discards the elements once the fixed point is reached. The high dispersions in H_{BPW} , C_{BPW} and MP are related to the short length of series' transient.

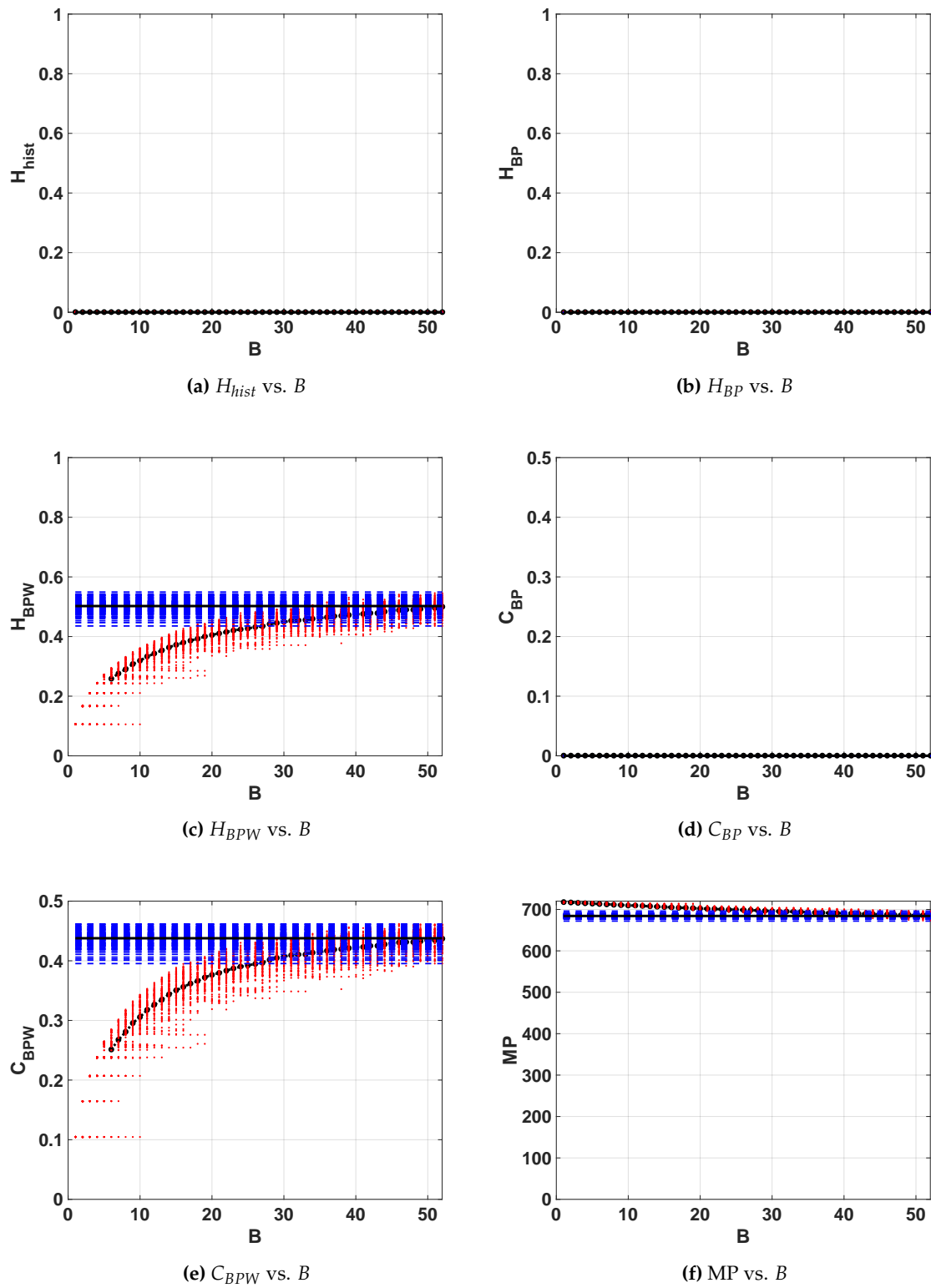


Figure 8. Statistical properties of TENT map.

351 Summarizing, in spite of using a high number of bits (with any 2-based numerical representation)
 352 to represent the digitalized TENT map it always converges to the fixed point in $(x_n, x_{n+1}) = (0, 0)$ after

³⁵³ a short transient. These transients have a maximum length of B elements (iterations) for fixed-point
³⁵⁴ arithmetic and 53 for floating-point (IEEE754 double precision).

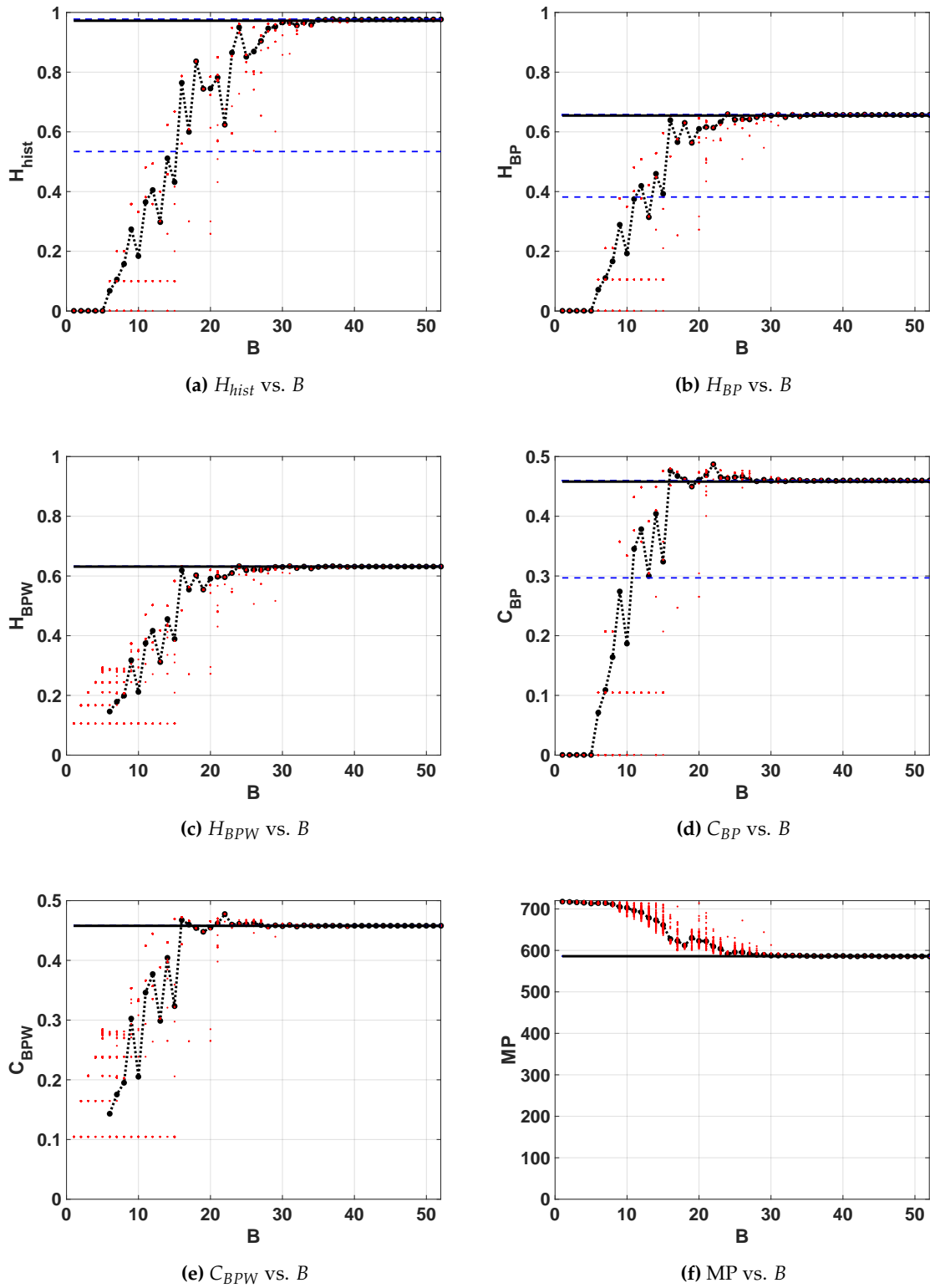
³⁵⁵ 3.3. *Quantifiers of combined Maps*

³⁵⁶ Here we report our results for the three combinations of the combined maps, SWITCH, EVEN
³⁵⁷ and ODD.

³⁵⁸ 3.3.1. SWITCH

³⁵⁹ Results with sequential switching are shown in Figures 9a to 9f. The calculated entropy value for
³⁶⁰ floating-point implementation is $\langle H_{hist} \rangle = 0.9722$, this value is slightly higher than the one obtained for
³⁶¹ the LOG map. For fixed-point arithmetic this value is reached in $B = 24$, but it stabilizes from $B = 28$.
³⁶² Regarding the ordering patterns the number of MP decreases to 586, this value is lower than the one
³⁶³ obtained for LOG map. It means the entropy H_{BP} may increase up to $\ln(134) / \ln(720) \simeq 0.74$. BP and
³⁶⁴ BPW quantifiers reach their maximum of $\langle H_{BP} \rangle = 0.6546$ and $\langle H_{BPW} \rangle = 0.6313$ at $B = 16$, but they
³⁶⁵ stabilize from $B = 24$. Complexities are lower than for LOG, $\langle C_{BP} \rangle = 0.4580$ and $\langle C_{BPW} \rangle = 0.4578$,
³⁶⁶ these values are reached for $B \geq 15$ but they stabilize for $B \geq 23$. Compared with LOG, statistical
³⁶⁷ properties are better with less amount of bits, for $B \geq 24$ this map reaches optimal characteristics in
³⁶⁸ the sense of random source.

³⁶⁹ Furthermore, we encountered one initial condition in floating-point with an anomalous behavior.
³⁷⁰ Figures 9a, 9b and 9d show an horizontal blue dashed line that is far from the average value, unlike this
³⁷¹ is not detected by quantifiers based on BPW procedure in Figures 9c and 9e. Nevertheless comparing
³⁷² both procedures (BP and BPW) we were able to detect a falling to fixed point after a long transitory,
³⁷³ the BPW procedure discards the constant values (corresponding with a fixed point) and works only
³⁷⁴ over the transitory values.

**Figure 9.** Statistical properties of SWITCH map.

375 Double entropy plane $H_{hist} \times H_{BP}$ is showed in Figures 10. The reached point in this plane for
 376 SWITCH map is similar to that reached for LOG map, and it is denoted by a star in the figure. The
 377 mixing is slight better in this case.

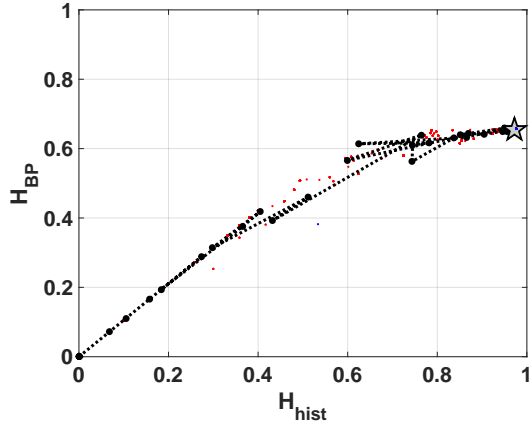


Figure 10. Evolution of statistical properties in double entropy plane for SWITCH map $H_{hist} \times H_{BP}$.

378 Entropy-complexity plane $H_{BP} \times C_{BP}$ is showed in Figures 11. If we compare with the same plane
 379 in the case of LOG (Figures 7a), C_{BP} is lower for SWITCH, this fact shows a more random behavior.

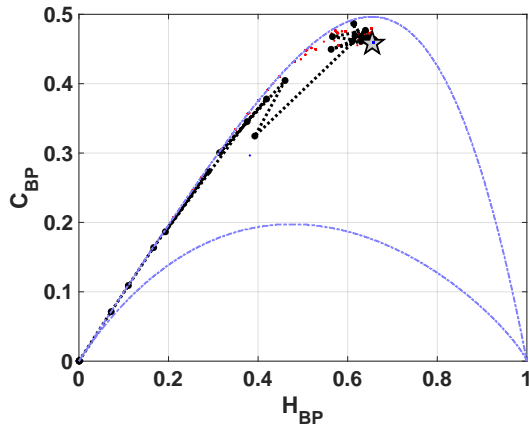


Figure 11. Evolution of statistical properties in causal entropy-complexity plane for SWITCH map $H_{BP} \times C_{BP}$.

380 3.3.2. EVEN and ODD

381 In Figures 12a and 13a we can see that quantifiers related to the normalized histogram of values
 382 slightly degrades with the skipping procedure. For example $\langle H_{hist} \rangle$ reduces from 0.9722 without
 383 skipping to 0.9459 for EVEN and 0.9706 for ODD. This difference between EVEN and ODD in floating
 384 point is because a high dispersion was obtained for H_{hist} , H_{BP} and C_{BP} but not for H_{BPW} or C_{BPW} .

385 Figures 12b to 12f and Figures 13b to 13f show the results of BP and BPW quantifiers for EVEN
 386 and ODD respectively. Higher accuracy is required to achieve lower complexity than without using
 387 skipping. From the MP point of view a great improvement is obtained using any of the skipping
 388 strategies but ODD is slightly better than EVEN. Missing patterns are reduced to $MP = 118$ for EVEN
 389 and ODD, increasing the maximum allowed Bandt & Pompe entropy that reaches the mean value
 390 $\langle H_{BP} \rangle = 0.8381$ for EVEN, and $\langle H_{BP} \rangle = 0.9094$. The complexity is reduced to $\langle C_{BP} \rangle = 0.224$ for EVEN
 391 and $\langle C_{BP} \rangle = 0.282$ for ODD. The minimum number of bits to converge to this value is $B > 40$ for both
 392 EVEN and ODD maps.

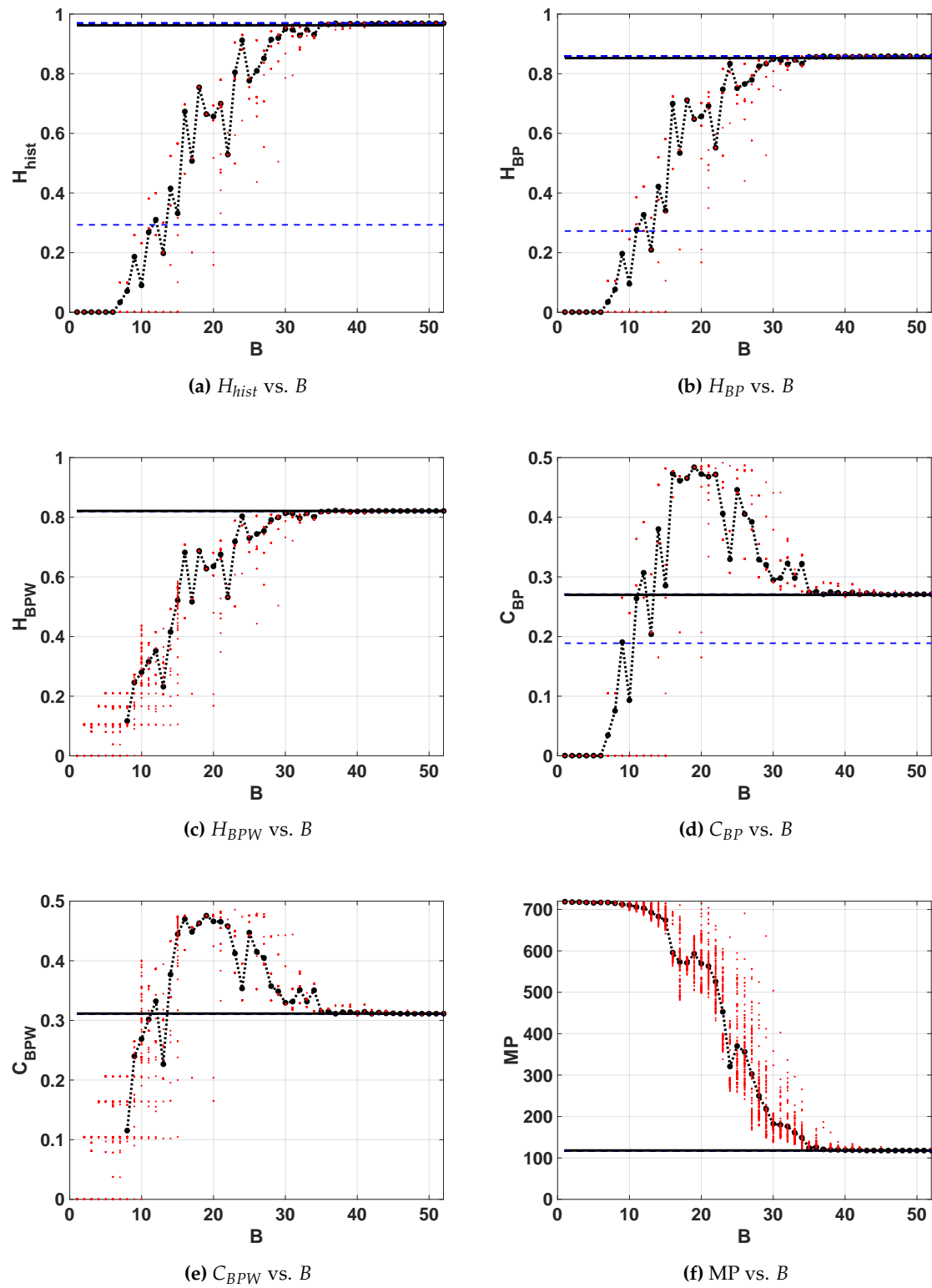
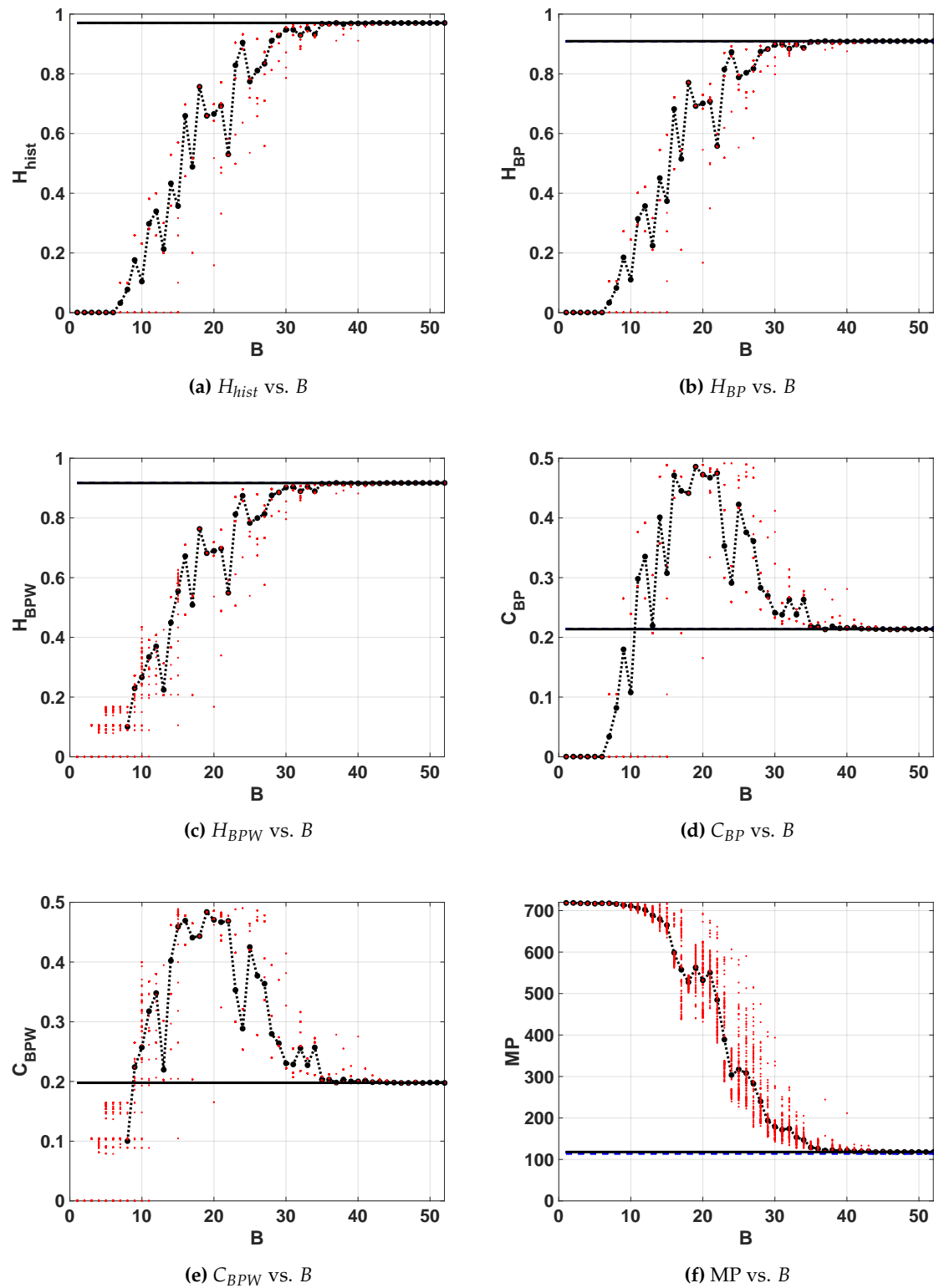


Figure 12. Statistical properties of EVEN map.

**Figure 13.** Statistical properties of ODD map.

³⁹³ The enhancement showed in Figures 12 and 13 is reflected in the position of asymptotic point
³⁹⁴ in the planes 14, and 15. In both cases this position is closest to the ideal point $(H_{hist}, H_{BP}) = (1, 1)$,
³⁹⁵ because the resulting vectors present better mixing.

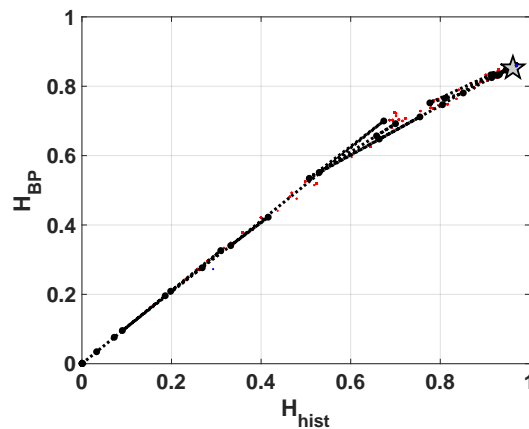


Figure 14. Evolution of statistical properties in double entropy plane for EVEN map $H_{hist} \times H_{BP}$.

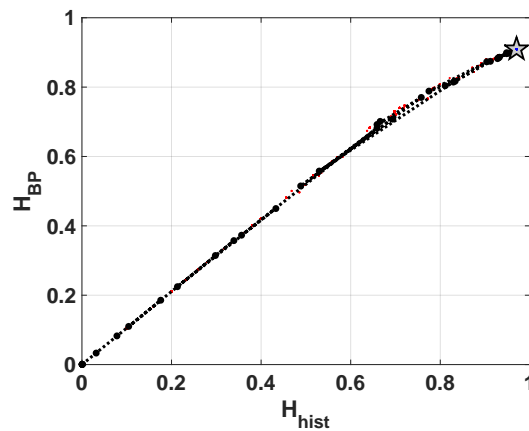


Figure 15. Evolution of statistical properties in double entropy plane for ODD map $H_{hist} \times H_{BP}$.

396 Compatible results are shown in Figures 16 and 17, the position of asymptotic point is closest to
 397 the ideal point $(H_{hist}, H_{BP}) = (1, 0)$. This result reflects that mixing is better because the complexity
 398 of resulting system is lower. This plane detects that the vector generated by ODD skipping is more
 399 mixed than EVEN.

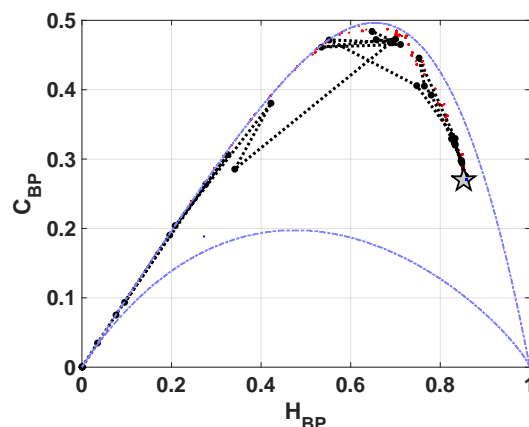


Figure 16. Evolution of statistical properties in entropy-complexity plane for EVEN map $H_{BP} \times C_{BP}$.

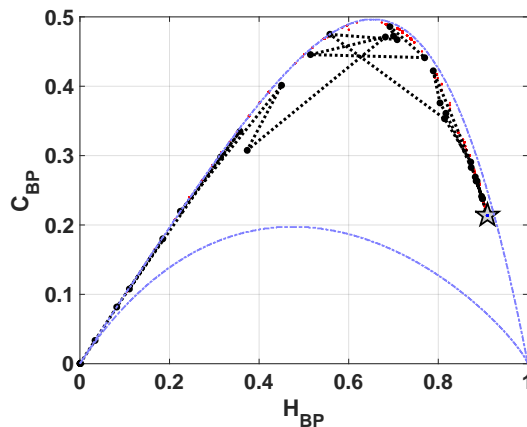


Figure 17. Evolution of statistical properties in entropy-complexity plane for ODD map $H_{BP} \times C_{BP}$.

400 4. Conclusions

401 In this paper we explored the statistical degradation of simple, switched and skipped chaotic
 402 maps due to the inherent error of a based-2 systems. We evaluated mixing and amplitude distributions
 403 from a statistical point of view.

404 Our work complements previous results given in [13], where period lengths were investigated. In
 405 that sense, our results were compatible with these. We can see that the switching between two maps
 406 increases the dependence of period as function of precision, this is because the correlation length is
 407 also increased. Nevertheless, the standard procedure of skipping reduce the period length in almost a
 408 half.

409 All statistics of the maps represented in fixed-point produces a non-monotonous evolution toward
 410 the floating-point results. This result is relevant because it shows that increasing the precision is not
 411 always recommended.

412 It is specially interesting to note that some systems (TENT) with very nice statistical properties in
 413 the real numbers world, become "pathological" when binary numerical representations are used. As a
 414 rule, if a map is generated only by shift operations (it depends on the base of the arithmetic logic unit
 415 and the map itself), all initial conditions will converge to a fixed point with a transient no longer than
 416 the length of the mantissa being used.

417 By comparing between BP and BPW quantifiers, we were able to detect falls to fixed points and to
 418 estimate the relative length of transient. It can be seen in all implementations of TENT, in one initial
 419 condition of SWITCH and EVEN for floating-point implementation.

420 Related to statistical behavior, our results show that SWITCH has a marginal improvement in
 421 the mixing with respect to LOG (and TENT, of course). However the greatest improvement comes
 422 when skipping is applied, we can see that BP and BPW entropies grow and BP and BPW complexities
 423 decrease, for the same numerical representation. This result is relevant because evidences that a long
 424 period is not synonymous of good statistics, switched maps EVEN and ODD have half period lengths
 425 but their mixing is better and their amplitude distributions remain almost equal. As counterpart, more
 426 precision is needed to reach the better asymptotes that offers the switching method.

427 **Acknowledgments:** This work was partially supported by the Consejo Nacional de Investigaciones Científicas y
 428 Técnicas (CONICET), Faculty of Engineering of the National University of Mar del Plata (FI-UNMDP) and the
 429 International Centre for Theoretical Physics (ICTP) Associateship Scheme.

430 References

- 431 1. Machado, R.F.; Baptista, M.S.; Grebogi, C. Cryptography with chaos at the physical level. *Chaos, Solitons
 432 and Fractals* **2004**, *21*, 1265–1269.

- 433 2. Smaoui, N.; Kanso, A. Cryptography with chaos and shadowing. *Chaos, Solitons and Fractals* **2009**,
434 42, 2312–2321.
- 435 3. De Micco, L.; Antonelli, M.; Larrondo, H. Stochastic degradation of the fixed-point version of 2D-chaotic
436 maps. *Chaos, Solitons and Fractals* **2017**, *104*, 477–484.
- 437 4. Antonelli, M.; Micco, L.D.; Gonzalez, C.M.; Larrondo, H.A. Analysis of the digital implementation of a
438 chaotic deterministic-stochastic attractor. 2012 Argentine School of Micro-Nanoelectronics, Technology
439 and Applications (EAMTA), 2012, pp. 73–78.
- 440 5. De Micco, L.; Petrocelli, R.A.; Larrondo, H.A. Constant Envelope Wideband Signals using Arbitrary
441 Chaotic Maps. *Proceedings of XII RPIC 2007*.
- 442 6. De Micco, L.; Arizmendi, C.M.; Larrondo, H.A. Zipping characterization of chaotic sequences used in
443 spread spectrum communication systems. *Institute of Physics Conference Proceedings 913* **2007**, pp. 139–144.
- 444 7. Alcover, P.M. Moiré interferences in the map of orbits of the Mandelbrot Set. *Commun. Nonlinear Sci.
445 Numer. Simul.* **2017**, *42*, 545–559.
- 446 8. Dias, S.P.; Longa, L.; Curado, E. Influence of the finite precision on the simulations of discrete dynamical
447 systems. *Commun. Nonlinear Sci. Numer. Simul.* **2011**, *16*, 1574–1579.
- 448 9. Azzaz, M.S.; Tanougast, C.; Sadoudi, S.; Bouridane, A. Synchronized hybrid chaotic generators: Application
449 to real-time wireless speech encryption. *Commun. Nonlinear Sci. Numer. Simul.* **2013**, *18*, 2035–2047.
- 450 10. Nepomuceno, E.G.; Mendes, E.M. On the analysis of pseudo-orbits of continuous chaotic nonlinear systems
451 simulated using discretization schemes in a digital computer. *Chaos, Solitons and Fractals* **2017**, *95*, 21–32.
- 452 11. Grebogi, C.; Ott, E.; Yorke, J.A. Roundoff-induced periodicity and the correlation dimension of chaotic
453 attractors. *Phys. Rev. A* **1988**, *38*, 3688–3692.
- 454 12. Persohn, K.J.; Povinelli, R.J. Analyzing logistic map pseudorandom number generators for periodicity
455 induced by finite precision floating-point representation. *Chaos, Solitons and Fractals* **2012**, *45*, 238–245.
- 456 13. Nagaraj, N.; Shastry, M.C.; Vaidya, P.G. Increasing average period lengths by switching of robust chaos
457 maps in finite precision. *Eur. Phys. J. Spec. Top.* **2008**, *165*, 73–83.
- 458 14. Liu, X.; Teo, K.L.; Zhang, H.; Chen, G. Switching control of linear systems for generating chaos. *Fractals An
459 Interdiscip. J. Complex Geom. Nat.* **2006**, *30*, 725–733.
- 460 15. Gluskin, E. The nonlinear-by-switching systems (a heuristic discussion of some basic singular systems)
461 **2008**. [[0801.3652](#)].
- 462 16. Zarlenga, D.G.; Larrondo, H.A.; Arizmendi, C.M.; Family, F. Complex synchronization structure of an
463 overdamped ratchet with discontinuous periodic forcing. *Phys. Rev. E - Stat. Nonlinear, Soft Matter Phys.*
464 **2009**, *80*, 011127.
- 465 17. Chiou, J.S.; Cheng, C.M. Stabilization analysis of the switched discrete-time systems using Lyapunov
466 stability theorem and genetic algorithm. *Chaos, Solitons and Fractals* **2009**, *42*, 751–759.
- 467 18. Borah, M.; Roy, B.K. An enhanced multi-wing fractional-order chaotic system with coexisting attractors
468 and switching hybrid synchronisation with its nonautonomous counterpart. *Chaos, Solitons and Fractals*
469 **2017**, *102*, 372–386.
- 470 19. De Micco, L.; Larrondo, H.A.; Plastino, A.; Rosso, O.A. Quantifiers for randomness of chaotic
471 pseudo-random number generators. *Philos. Trans. A. Math. Phys. Eng. Sci.* **2009**, *367*, 3281–3296,
472 [[0812.2250](#)].
- 473 20. Bandt, C.; Pompe, B. Permutation entropy: a natural complexity measure for time series. *Phys. Rev. Lett.*
474 **2002**, *88*, 174102.
- 475 21. De Micco, L.; González, C.M.; Larrondo, H.A.; Martin, M.T.; Plastino, A.; Rosso, O.A. Randomizing
476 nonlinear maps via symbolic dynamics. *Phys. A Stat. Mech. its Appl.* **2008**, *387*, 3373–3383.
- 477 22. De Micco, L.; Fernández, J.G.; Larrondo, H.A.; Plastino, A.; Rosso, O.A. Sampling period, statistical
478 complexity, and chaotic attractors. *Phys. A Stat. Mech. its Appl.* **2012**, *391*, 2564–2575.
- 479 23. Rosso, O.A.; Larrondo, H.A.; Martin, M.T.; Plastino, A.; Fuentes, M.A. Distinguishing noise from chaos.
480 *Phys. Rev. Lett.* **2007**, *99*, 154102, [[1401.2139](#)].
- 481 24. Rosso, O.A.; De Micco, L.; Larrondo, H.A.; Martin, M.T.; Plastino, A. Generalized Statistical Complexity
482 Measure. *Int. J. Bifurc. Chaos* **2010**, *20*, 775.
- 483 25. Antonelli, M.; De Micco, L.; Larrondo, H.A. Measuring the jitter of ring oscillators by means of information
484 theory quantifiers. *Commun. Nonlinear Sci. Numer. Simul.* **2017**, *43*, 139–150.

- 485 26. Fadlallah, B.; Chen, B.; Keil, A.; Príncipe, J. Weighted-permutation entropy: A complexity measure for time
486 series incorporating amplitude information. *Phys. Rev. E - Stat. Nonlinear, Soft Matter Phys.* **2013**, *87*, 1–7.
- 487 27. Amigó, J.M.; Zambrano, S.; Sanjuán, M.A.F. True and false forbidden patterns in deterministic and random
488 dynamics. *Europhys. Lett.* **2007**, *79*, 50001.
- 489 28. Rosso, O.A.; Carpi, L.C.; Saco, P.M.; Ravetti, M.G.; Larrondo, H.A.; Plastino, A. The Amigo paradigm of
490 forbidden/missing patterns: A detailed analysis. *Eur. Phys. J. B* **2012**, *85*.
- 491 29. Shannon, C.E.; Weaver, W. The mathematical theory of communication. *Bell Syst. Tech. J.* **1948**, *27*, 379–423.
- 492 30. Kantz, H.; Kurths, J.; G., M.K. *Nonlinear Analysis of Physiological Data* / Springer Science & Business Media;
493 Springer, 2012; p. 344.
- 494 31. Feldman, D.P.; McTague, C.S.; Crutchfield, J.P. The organization of intrinsic computation: Complexity-entropy diagrams and the diversity of natural information processing. *Chaos* **2008**, *18*, 043106,
495 [0806.4789].
- 496 32. Lamberti, P.W.; Martin, M.T.; Plastino, A.; Rosso, O.A. Intensive entropic non-triviality measure. *Phys. A Stat. Mech. its Appl.* **2004**, *334*, 119–131.
- 497 33. López-Ruiz, R.; Mancini, H.L.; Calbet, X.; Lpez-Ruiz, R.; Mancini, H.L.; Calbet ', X. A statistical measure
498 of complexity. *Phys. Lett. A* **1995**, *209*, 321–326.
- 499 34. Martin, M.T.; Plastino, A.; Rosso, O.A. Statistical complexity and disequilibrium. *Phys. Lett. Sect. A Gen. At. Solid State Phys.* **2003**, *311*, 126–132.
- 500 35. Grossé, I.; Bernaola-Galván, P.; Carpena, P.; Romón-Roldán, R.; Oliver, J.; Stanley, H.E. Analysis of symbolic
501 sequences using the Jensen-Shannon divergence. *Phys. Rev. E. Stat. Nonlin. Soft Matter Phys.* **2002**, *65*, 16.
- 502 36. Martin, M.T.; Plastino, A.; Rosso, O.A. Generalized statistical complexity measures: Geometrical and
503 analytical properties. *Phys. A Stat. Mech. its Appl.* **2006**, *369*, 439–462.
- 504 37. Rosso, O.A.; Zunino, L.; Pérez, D.G.; Figliola, A.; Larrondo, H.A.; Garavaglia, M.; Martín, M.T.; Plastino, A.
505 Extracting features of Gaussian self-similar stochastic processes via the Bandt-Pompe approach. *Phys. Rev. E - Stat. Nonlinear, Soft Matter Phys.* **2007**, *76*, 061114.
- 506 38. Anteneodo, C.; Plastino, A.R. Some features of the López-Ruiz-Mancini-Calbet (LMC) statistical measure
507 of complexity. *Phys. Lett. Sect. A Gen. At. Solid State Phys.* **1996**, *223*, 348–354.
- 508 39. Olivares, F.; Plastino, A.; Rosso, O.A. Contrasting chaos with noise via local versus global information
509 quantifiers, 2012.
- 510 40. González, C.M.; Larrondo, H.A.; Rosso, O.A. Statistical complexity measure of pseudorandom bit
511 generators. *Phys. A Stat. Mech. its Appl.* **2005**, *354*, 281–300.
- 512 41. Amigó, J.M.; Kocarev, L.; Szczepanski, J. Order patterns and chaos. *Phys. Lett. Sect. A Gen. At. Solid State
513 Phys.* **2006**, *355*, 27–31.
- 514 42. Amigó, J.M.; Kocarev, L.; Tomovski, I. Discrete entropy. *Phys. D Nonlinear Phenom.* **2007**, *228*, 77–85.
- 515 43. Amigó, J.M.; Zambrano, S.; Sanjuán, M.A.F. Combinatorial detection of determinism in noisy time series.
516 *Europhys. Lett.* **2008**, *83*, 60005.
- 517 44. Amigó, J. *Permutation Complexity in Dynamical Systems*; Springer Series in Synergetics, Springer Berlin
518 Heidelberg: Berlin, Heidelberg, 2010; pp. 195–197, [arXiv:1011.1669v3].
- 519 45. De Micco, L.; Antonelli, M.; Larrondo, H.A.; Boemo, E. Ro-based PRNG: FPGA implementation and
520 stochastic analysis. 2014 9th South. Conf. Program. Logic, SPL 2014. IEEE, 2015, pp. 1–6.
- 521 46. Wackerbauer, R.; Witt, A.; Atmanspacher, H.; Kurths, J.; Scheingraber, H. A comparative classification of
522 complexity measures. *Chaos, Solitons and Fractals* **1994**, *4*, 133–173.
- 523 47. Antonelli, M.; De Micco, L.; Larrondo, H. Causal and non-causal entropy quantifiers implemented in
524 FPGA. 2016 IEEE Bienn. Congr. Argentina, ARGENCON 2016. IEEE, 2016, pp. 1–5.
- 525 48. Lasota, A.; Mackey, M.C. *Chaos, fractals, and noise : stochastic aspects of dynamics*; Number 97, Springer-Verlag,
526 1994; pp. xiv, 472 p.
- 527 49. Jessa, M. The period of sequences generated by tent-like maps. *IEEE Trans. Circuits Syst. I Fundam. Theory
528 Appl.* **2002**, *49*, 84–89.
- 529 50. Callegari, S.; Setti, G.; Langlois, P. A CMOS tailed tent map for the generation of uniformly distributed
530 chaotic sequences. Proc. 1997 IEEE Int. Symp. Circuits Syst. Circuits Syst. Inf. Age ISCAS '97. IEEE, 2013,
531 Vol. 2, pp. 781–784, [1302.0511].
- 532 51. Li, S. When Chaos Meets Computers, 2004, [arXiv:nlin/0405038].

⁵³⁷ © 2017 by the authors. Submitted to *Entropy* for possible open access publication under the terms and conditions
⁵³⁸ of the Creative Commons Attribution (CC BY) license (<http://creativecommons.org/licenses/by/4.0/>).